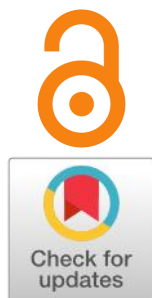


A comprehensive study of the thermal behavior of rare earth chloride hydrates: resolving contradictions

Irina Zakiryanova^{a*}, Iraida Korzun^a, Emma Vovkotrub^a, Boris Antonov^aReceived: 11 January 2024
Accepted: 12 February 2024
Published online: 6 March 2024DOI: [10.15826/elmattech.2024.3.028](https://doi.org/10.15826/elmattech.2024.3.028)

Rare earth metal chlorides are used as starting materials on electrochemical synthesis of pure metals. These chlorides are hygroscopic and tend to form hydrates. To resolve the uncertainty of the thermal behavior of the hydrates $\text{LaCl}_3 \cdot 7\text{H}_2\text{O}$, $\text{NdCl}_3 \cdot 6\text{H}_2\text{O}$, $\text{SmCl}_3 \cdot 6\text{H}_2\text{O}$, and $\text{YbCl}_3 \cdot 6\text{H}_2\text{O}$, a comprehensive study is carried out. Thermogravimetry, differential scanning calorimetry and mass spectrometry were used to reveal the dehydration and hydrolysis processes over the temperature range of 25–700 °C. Phase compositions of the initial hydrates, intermediate and final products are investigated by the XRD analysis, Raman and IR spectroscopy. Distinctions in the thermal behavior of the studied hydrates were found. The features must be taken into account when obtaining anhydrous rare earth chlorides and in technological processes with its participation.

keywords: dehydration, hydrolysis, rare earth chloride, oxychloride, hydrates, thermal analysis, mass spectrometry, Raman spectra, IR spectra

© 2024, the Authors. This article is published in open access under the terms and conditions of the Creative Commons Attribution (CC BY) license <http://creativecommons.org/licenses/by/4.0/>.

1. Introduction

Rare earth metals (*REMs*) and mish metals are widely used in various fields of production, technology and medicine. In particular, lanthanum and neodymium participate in aluminum, magnesium, titanium and other alloys which are used in aviation and rocket production. Lanthanum is used in nickel-hydride batteries. Lanthanum glasses are exploited to lenses of photographic equipment and astronomical instruments. Samarium is used as an activator of phosphors for TV and cell phone screens. Mish metals Sm-Co and Nd-Fe are included in the materials for the manufacture of powerful permanent magnets. Gadolinium alloys with cobalt and iron have unique magnetic properties and are

used to create high-density memory media. Ytterbium is one of the most sought *REMs* required for the optical applications. It is part of the optical fiber of today's most powerful IR lasers. Materials with ytterbium are used for improving the efficiency of silicon solar cells. Phosphors containing ytterbium ions have been successfully applied to convert X-rays into visible light, which can significantly reduce the radiation dose required to obtain medical X-ray images. Preparations based on ytterbium-169 are used in nuclear medicine for diagnostic procedures and radiotherapy [1–4].

The main method of obtaining *REMs* is the thermal reduction of *REM* oxides, chlorides, or fluorides with calcium [3]. At the same time, research is being conducted aimed at developing the electrochemical synthesis using molten salt media [5–7]. *REM* chlorides can be used as starting materials. Lanthanum, cerium, neodymium, praseodymium, samarium, and yttrium have been successfully obtained by electrochemical reduction. These studies often noted difficulties in carrying out the electrolysis associated with the

a: Institute of High-Temperature Electrochemistry of the Ural Branch of the Russian Academy of Sciences, Ekaterinburg 620066, Russian Federation

* Corresponding author: optic96@mail.ru

hydrolysis of *REM* chlorides in the presence of atmospheric moisture. This feature imposes certain requirements on the handling of raw materials and the electrolyzer design.

REM chlorides are hygroscopic, actively absorb water, turning into crystal hydrates $REMCl_3 \cdot nH_2O$. On heating, the formation of oxychlorides is possible [8–10]. The presence of undesirable oxygen-containing impurities can lead to changes in the physicochemical properties of the electrolyte and has a negative impact on ongoing high-temperature electrochemical processes and the yield of target components [3, 7, 11–15].

Up to now the information on the processes of thermal dehydration of the *REM* chlorides hydrates, the composition of intermediate and final phases is contradictory [8, 9, 16–25].

In particular, work [8] presents results of studying the thermal decomposition process of the hydrate $SmCl_3 \cdot 6H_2O$ in an air atmosphere using thermogravimetry (TG). The authors note that the thermal dehydration of $SmCl_3 \cdot 6H_2O$ begins at 85 °C. When the sample is heated up to 195 °C the mass decreases, and the formation of $SmCl_3 \cdot H_2O$ monohydrate occurs. At 250 °C anhydrous salt $SmCl_3$ and an admixture of $SmOCl$ oxychloride are formed. On heating up to 505 °C the subsequent decrease in the mass is attended by the transformation of the anhydrous salt to $SmOCl$. A similar scheme of thermal dehydration has been proposed for hydrates $NdCl_3 \cdot 6H_2O$, $GdCl_3 \cdot 6H_2O$, $YCl_3 \cdot 6H_2O$ [8]. It should be noted that the authors' assumptions about changes in the hydrates phase composition during thermal dehydration are based on the TG measurements only. Phase analysis was not performed.

In [16], the process of $SmCl_3 \cdot 6H_2O$ thermal decomposition in an inert atmosphere (N_2) was studied using differential scanning calorimetry (DSC). Based on the obtained caloric effects, the authors propose a thermal dehydration scheme other than [8], namely: $SmCl_3 \cdot 6H_2O \rightarrow SmCl_3 \cdot 4H_2O \rightarrow SmCl_3 \cdot 2H_2O \rightarrow SmCl_3 \cdot H_2O \rightarrow SmCl_3$. It was noted that the final product (anhydrous $SmCl_3$) is formed at 250 °C. The formation of an intermediate dehydration product (hydrate $LnCl_3 \cdot 4H_2O$) was also found when heating $LnCl_3 \cdot 6H_2O$ ($Ln = Tb, Er, Tm, Yb, Lu$) [16]. However, the studies [17–19] on the temperature dependence of the equilibrium pressure of water vapor over compounds $LnCl_3 \cdot 6H_2O$ ($Ln = Sm, Eu, Nd, Gd, Er, Tm, Lu$), supplemented by TG measurements, showed that all studied crystalline hydrates lose 3 moles of water per 1 mole of substance at the first step of dehydration,

forming hydrates $LnCl_3 \cdot 3H_2O$. Hydrates $LnCl_3 \cdot 4H_2O$ were not found.

The work [21] presents the results of a study of the thermal behavior of *REM* chloride hydrates carried out by an original technique, including blowing a mixture of gases (Ar and HCl) over the samples. The resulting thermal dehydration schemes are partially consistent with deductions [16] and [17–18].

The work [22] presents the results of synchronous thermal analysis (STA) which includes TG simultaneously with DSC measurements of *REM* chloride hydrates. The experiments were carried out in an argon atmosphere, heating the samples up to 230 °C. The authors' conclusions contradict the deductions of the works [8, 9, 16–21]. For example, the dehydration scheme for samarium chloride hydrate has been proposed: $SmCl_3 \cdot 7.8H_2O \rightarrow SmCl_3 \cdot 3.6H_2O \rightarrow SmCl_3 \cdot 2.0H_2O \rightarrow SmCl_3 \cdot 0.4H_2O$. It should be noted that the temperatures of TG and DSC effects do not agree with those indicated on the dehydration schemes [22].

A significant drawback of all the studies mentioned is, in our opinion, the lack of information on the certification of the initial samples, the insufficient validity of conclusions about the composition of the intermediate and final products and the steps of dehydration and hydrolysis. Finally, a general lack of an integrated approach can be noted when studying these processes.

Recently, we studied [10] the process of thermal dehydration of hydrate $GdCl_3 \cdot 6H_2O$, carrying out simultaneously TG, DSC measurements and mass spectrometry analysis (MSA) of the exit gases. The initial samples and final products of thermal decomposition were certified by XRD analysis, Raman and IR spectroscopy. When $GdCl_3 \cdot 6H_2O$ is heated the decomposition process was shown to occur according to the following scheme: $GdCl_3 \cdot 6H_2O \rightarrow GdCl_3 \cdot 3H_2O \rightarrow GdCl_3 \cdot 2H_2O \rightarrow GdCl_3 \cdot H_2O \rightarrow GdCl_3 + GdOCl \rightarrow GdOCl$. It has been established that over a temperature range of 200–275 °C the formation of an anhydrous salt is accompanied by hydrolysis. As a result, oxychloride $GdOCl$ is formed. In the presence of water vapor at 300–370 °C anhydrous salt hydrolyzes, turning into oxychloride. Based on the results of DSC measurements and thermodynamic modeling, an assessment was made of the thermal effects accompanying the ongoing chemical reactions.

In this study we present the results of a comprehensive study of the thermal behavior of hydrates $LaCl_3 \cdot 7H_2O$, $NdCl_3 \cdot 6H_2O$, $SmCl_3 \cdot 6H_2O$ and $YbCl_3 \cdot 6H_2O$ using TG, DSC, MSA, XRD, Raman, and IR spectroscopy.

2. Experimental

2.1. Experimental techniques

Determination of the temperatures of phase transformations, accompanying thermal effects and mass spectrometric analysis of the exit gases were carried out on a synchronous thermal analyzer STA 449C Jupiter coupled with an Aeolos quadrupole mass spectrometer (NETZSCH, Germany). The instrument was calibrated using reference samples of RbNO_3 , KClO_4 , Ag_2SO_4 , CsCl , K_2CrO_4 and biphenyl $\text{C}_{10}\text{H}_{12}$ (NETZSCH). The mass of the initial samples was 10–13 mg, the heating rate was $5^\circ\text{C}/\text{min}$. The temperature range for thermal analysis was $25\text{--}700^\circ\text{C}$. To protect the device, measurements carried out in a flow of protective gas (high purity Ar, 99.998 %). The gas flow rate was 20 ml/min. The sample was placed in a Pt-Rh crucible with a pierced lid. According to the technical characteristics of the device, the error on determining the temperature was less than 1°C , the error on measuring mass was 10^{-6} g.

Certifications of the synthesized hydrates $\text{LaCl}_3 \cdot 7\text{H}_2\text{O}$, $\text{NdCl}_3 \cdot 6\text{H}_2\text{O}$, $\text{SmCl}_3 \cdot 6\text{H}_2\text{O}$ and $\text{YbCl}_3 \cdot 6\text{H}_2\text{O}$ and thermal decomposition products were carried out by XRD analysis, Raman and IR spectroscopy. X-ray patterns were recorded using an automatic X-ray diffractometer Rigaku D/MAX-2200VL/PC (Japan), equipped with a special attachment that allowed investigations to be carried out at elevated temperatures. The test samples are arranged on the attachment, evacuated, heated to designated temperature, and kept under isothermal conditions until a reproducible and stable X-ray pattern was obtained. This permits monitoring *in situ* changes in the phase composition of the samples on the temperature increasing. X-ray diffraction patterns were processed and phases were identified using MDI Jade 6.5 software.

IR spectra were recorded using the TENSOR 27 IR Fourier spectrometer (Bruker, Germany) over a range of $300\text{--}4000\text{ cm}^{-1}$. In preparation for IR analysis, samples were ground to fine powder in a vibrating mill and then pressed in a KBr matrix. Raman spectra were recorded using the UI000 Raman microscope-spectrometer (Renishaw, UK) over a range of $50\text{--}4000\text{ cm}^{-1}$. In this case no special sample preparation required. The sensitivities of the methods are 10^{-4} (IR) and 10^{-1} (Raman) mol % [26].

2.2. Synthesis and certification of hydrates $\text{REMCl}_3 \cdot n\text{H}_2\text{O}$ ($\text{REM} = \text{La, Nd, Sm, Yb}$)

Hydrates $\text{LaCl}_3 \cdot 7\text{H}_2\text{O}$, $\text{NdCl}_3 \cdot 6\text{H}_2\text{O}$, $\text{SmCl}_3 \cdot 6\text{H}_2\text{O}$ and $\text{YbCl}_3 \cdot 6\text{H}_2\text{O}$ were synthesized by the Reaction 1:



The oxides La_2O_3 – TU 48-4-523-90, Nd_2O_3 – TU 48-4-524-90, Sm_2O_3 – TU 48-4-523-90, Yb_2O_3 – TU 48-4-524-90 were pre-calcined at 1000°C in alundum crucibles in air atmosphere. Under this conditions, possible impurities in the form of $\text{REM}_2\text{O}_2\text{CO}_3$ and $\text{REM}(\text{OH})_3$ decompose to REM_2O_3 [27, 28]. Thereafter the REM oxide was transferred to a glassy carbon cup and dissolved in excess HCl_{conc} (CP).

The solution was evaporated, slowly heated to temperatures not exceeding 80°C . XRD of the obtained samples showed the formation of crystal hydrates with the following compositions: $\text{LaCl}_3 \cdot 7\text{H}_2\text{O}$, $\text{NdCl}_3 \cdot 6\text{H}_2\text{O}$, $\text{SmCl}_3 \cdot 6\text{H}_2\text{O}$ and $\text{YbCl}_3 \cdot 6\text{H}_2\text{O}$. As an example, Figure 1 presents the result of XRD certification of synthesized $\text{YbCl}_3 \cdot 6\text{H}_2\text{O}$.

The Raman spectrum of $\text{YbCl}_3 \cdot 6\text{H}_2\text{O}$ (Figure 2) shows vibration bands of medium intensity in the region of $60\text{--}400\text{ cm}^{-1}$, related to phonon modes; intense bands at 1634 , 3222 , 3336 and 3359 cm^{-1} , related to bending and stretching modes of the H_2O molecules in crystal lattice of hydrate, and bands of medium intensity at 613 and 677 cm^{-1} related to libration modes ones [29].

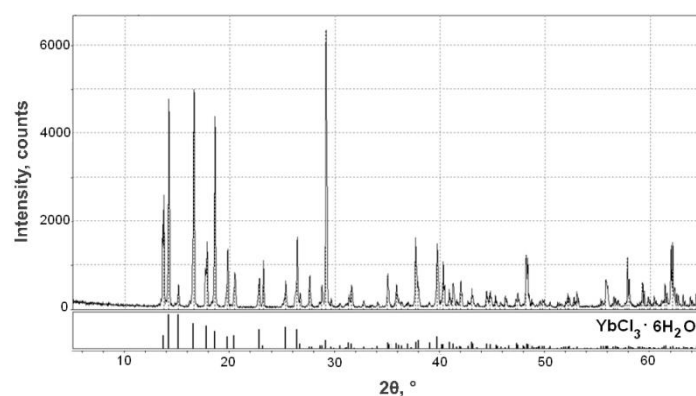


Figure 1 XRD analysis of synthesized $\text{YbCl}_3 \cdot 6\text{H}_2\text{O}$.

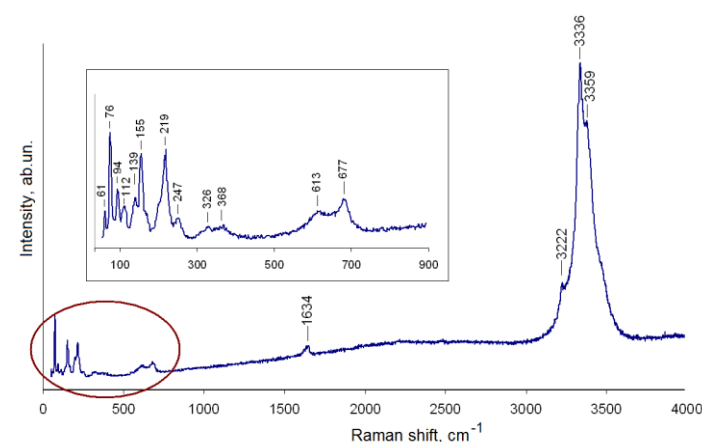


Figure 2 Raman spectrum of $\text{YbCl}_3 \cdot 6\text{H}_2\text{O}$. The inset shows the spectral region $50\text{--}900\text{ cm}^{-1}$ on an enlarged scale.

The results of the certification of the synthesized hydrate $\text{YbCl}_3 \cdot 6\text{H}_2\text{O}$ by X-ray diffraction confirmed the single-phase composition.

The Raman spectroscopy data indicate the absence of adsorbed water impurities, which presence can lead to additional caloric and gravimetric effects during STA measurements. Similar results were obtained on the certification of the synthesized hydrates $\text{LaCl}_3 \cdot 7\text{H}_2\text{O}$, $\text{NdCl}_3 \cdot 6\text{H}_2\text{O}$, $\text{SmCl}_3 \cdot 6\text{H}_2\text{O}$.

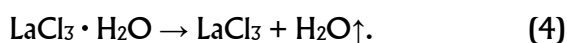
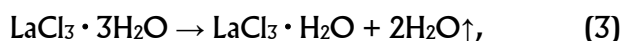
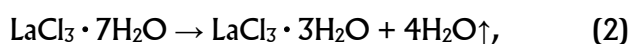
3. Results and discussion

3.1. $\text{LaCl}_3 \cdot 7\text{H}_2\text{O}$

Figure 3 shows the STA results for hydrate $\text{LaCl}_3 \cdot 7\text{H}_2\text{O}$. Three stages of weight loss accompanied by endothermic effects are detected over the temperature range of 25–200 °C.

On heating the $\text{LaCl}_3 \cdot 7\text{H}_2\text{O}$ up to 200 °C the weight loss is 31.7 wt. % corresponding the formation of anhydrous lanthanum chloride.

TG results showed the stepwise dehydration process by Reactions 2–4:



Over the temperature range of 300–600 °C a gradual weight loss accompanied by the endothermic effect was observed (Figure 3). We speculated that lanthanum chloride hydrolyzes in the presence of water vapor and turns into oxychloride LaOCl by the Reaction 5:

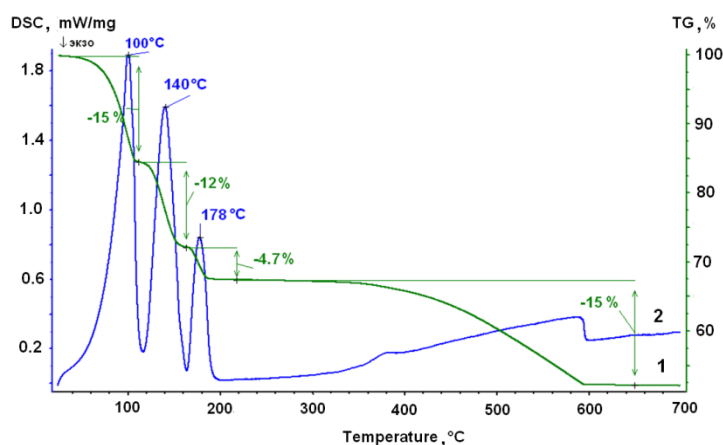


Figure 3 STA results on heating of $\text{LaCl}_3 \cdot 7\text{H}_2\text{O}$ (1 – weight, 2 – heat flow).

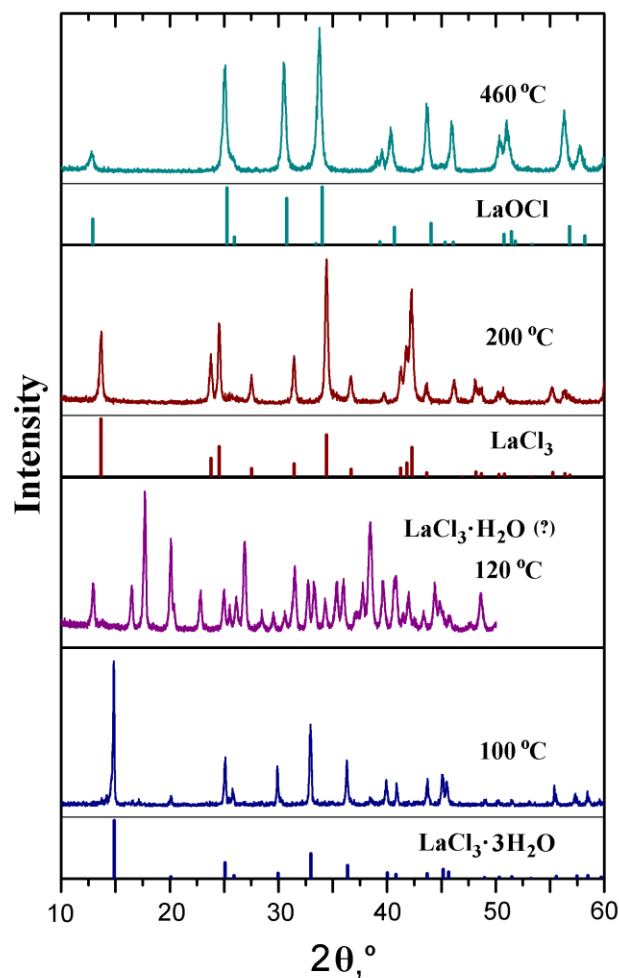


Figure 4 XRD results indicating the phase transformations during the thermal dehydration of lanthanum trichloride hydrate.

To verify the formation of intermediate hydrate phases, lanthanum chloride and oxychloride, the XRD analysis was carried out at elevated temperatures. Figure 4 shows the X-ray patterns and the identified phases.

According to the obtained XRD data, at 100 °C the sample is a single-phase hydrate $\text{LaCl}_3 \cdot 3\text{H}_2\text{O}$. Anhydrous LaCl_3 and oxychloride LaOCl were identified at 200 °C and 460 °C respectively. These results are in good agreement with the findings of STA. Unfortunately, we did not find the monohydrate $\text{LaCl}_3 \cdot \text{H}_2\text{O}$ X-ray diffraction pattern in the databases and therefore we cannot confirm the formation of this compound in the second step of the $\text{LaCl}_3 \cdot 7\text{H}_2\text{O}$ thermal dehydration. Nevertheless, Figure 4 shows the X-ray pattern of the sample at 120 °C, which presumably corresponds to the $\text{LaCl}_3 \cdot \text{H}_2\text{O}$. We point out the X-ray diffraction pattern of $\text{NdCl}_3 \cdot \text{H}_2\text{O}$ monohydrate [25] is closely similar.

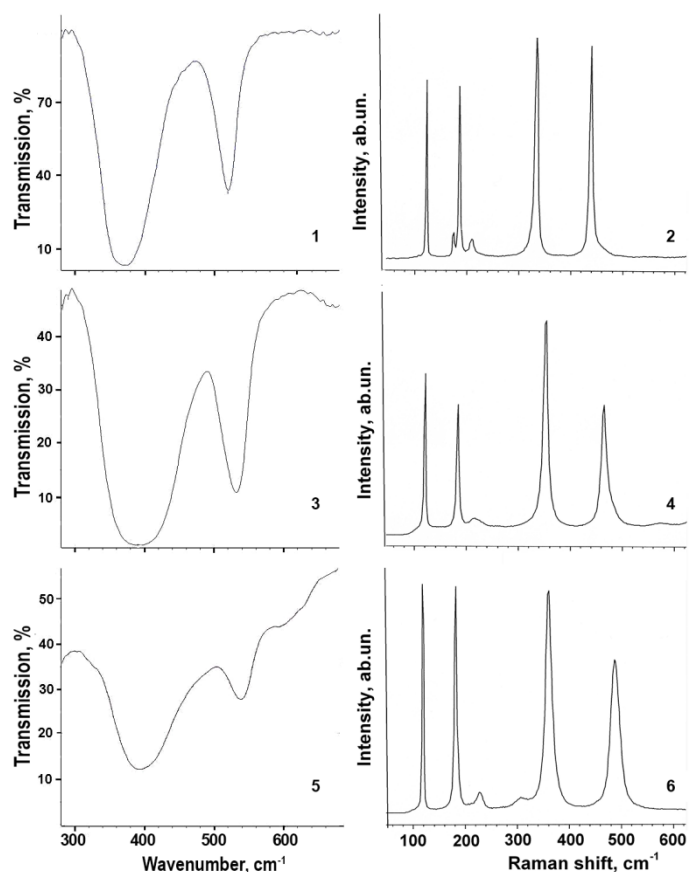


Figure 5 IR (1, 3, 5) and Raman (2, 4, 6) spectra of hydrolysis products: 1, 2 – LaOCl; 3, 4 – NdOCl; 5, 6 – SmOCl.

The formation of the oxychloride LaOCl during the hydrolysis of LaCl_3 was confirmed by Raman and IR spectroscopy. In the spectra of the sample after exposure of $\text{LaCl}_3 \cdot 7\text{H}_2\text{O}$ at 700°C under Ar atmosphere (Figure 5, curves 1 and 2) only vibration modes of LaOCl [30, 31] are presented (cm^{-1}): 121 – A_{1g} ; 185 – A_{1g} ; 210 – E_g ; 333 – B_g ; 438 – E_g ; 373 – A_{2u} ; 520 – E_u . Modes A_{1g} , E_g , B_g are active in the Raman spectrum, while A_{2u} and E_u are active in the IR spectrum. No vibration bands related to possible residual impurities of hydrates, adsorbed or crystallization water, and hydrogen chloride were detected.

Therefore, a comprehensive study performed with the STA, XRD, Raman and IR spectroscopy, established that the process of thermal decomposition of $\text{LaCl}_3 \cdot 7\text{H}_2\text{O}$ occurs in three steps and results in the formation of anhydrous LaCl_3 . Thermal dehydration proceeds according to the following scheme: $\text{LaCl}_3 \cdot 7\text{H}_2\text{O} \rightarrow \text{LaCl}_3 \cdot 3\text{H}_2\text{O} \rightarrow \text{LaCl}_3 \cdot \text{H}_2\text{O} \rightarrow \text{LaCl}_3$. Lanthanum chloride hydrolyzes and turns into LaOCl at temperatures above 300°C in the presence of water vapor.

3.2. $\text{NdCl}_3 \cdot 6\text{H}_2\text{O}$

In contrast to lanthanum chloride hydrate, in the case of $\text{NdCl}_3 \cdot 6\text{H}_2\text{O}$, DSC detected four endothermic

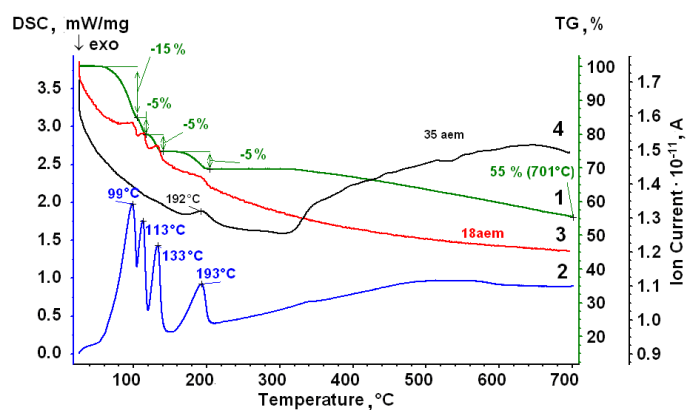
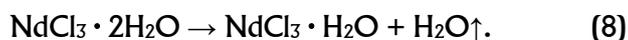
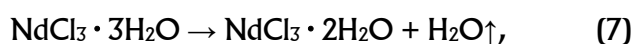
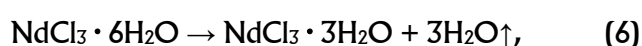


Figure 6 STA and MSA results on heating of $\text{NdCl}_3 \cdot 6\text{H}_2\text{O}$: 1 – weight, 2 – heat flow, 3 – H_2O ion current, 4 – HCl ion current.

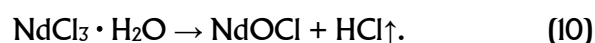
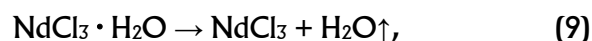
peaks (at 99, 113, 133 and 193°C) over the temperature range of $25\text{--}250^\circ\text{C}$. Endothermic effects are accompanied by the weight loss (Figure 6, curves 1 and 2). TG results could not give an unambiguous answer on the origin of the fourth endothermic peak and the phase composition of the sample.

To clarify the dehydration process of $\text{NdCl}_3 \cdot 6\text{H}_2\text{O}$, MSA of exit gases was carried out simultaneously with TG and DSC measurements. The results are shown in Figure 6 (curves 3 and 4).

Figure 6 shows that the thermal effects at 99, 113 and 133°C are accompanied by the exit of H_2O vapor, and the thermal effect at 193°C is accompanied by the exit of H_2O and HCl vapors. In accordance with TG, DSC and MSA data, the first three steps of dehydration are described by Reactions 6–8:



And in the fourth step (at 193°C), the formation of chloride NdCl_3 (Reaction 9) and oxychloride NdOCl (Reaction 10) occurs simultaneously:



On heating the sample above 300°C , weight loss and endothermic effect are accompanied by the exit of HCl vapors indicating the hydrolysis process by the Reaction 11:



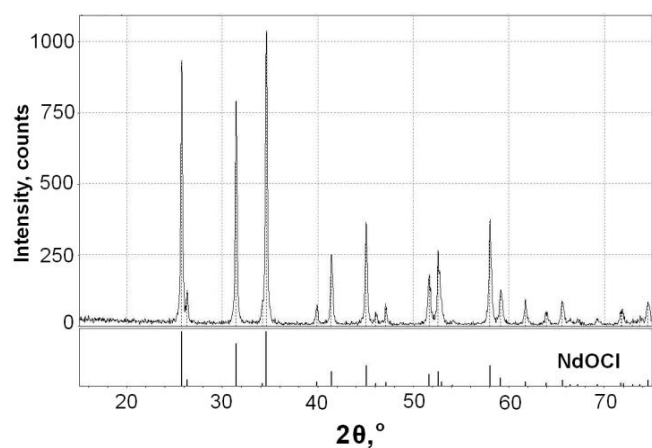
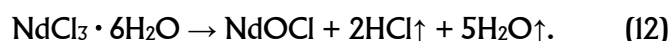


Figure 7 XRD analysis of the sample after 3-hour exposure of $\text{NdCl}_3 \cdot 6\text{H}_2\text{O}$ at $500\text{ }^\circ\text{C}$ under Ar atmosphere. Formation of the NdOCl is detected.

The formation of the neodymium oxychloride was confirmed by spectral investigations. Indeed, in the Raman and IR spectra of the sample (Figure 5, curves 3 and 4) after exposure of $\text{NdCl}_3 \cdot 6\text{H}_2\text{O}$ at $500\text{ }^\circ\text{C}$ under Ar atmosphere, the vibration modes of NdOCl [23, 24] were found (cm^{-1}): $119 - A_{1g}$; $182 - A_{1g}$; $217 - E_g$; $352 - B_g$; $464 - E_g$; $391 - A_{2u}$; $531 - E_u$. No vibration bands related to possible residual impurities of monohydrate $\text{NdCl}_3 \cdot \text{H}_2\text{O}$, adsorbed or crystallized H_2O , and HCl were detected. XRD analysis of the sample obtained by the same procedure confirmed the single-phase of the sample: only reflections of the NdOCl phase are present in the X-ray pattern (Figure 7).

Therefore, the formation of the final product (neodymium oxychloride) performed by two ways: hydrolysis of monohydrate $\text{NdCl}_3 \cdot \text{H}_2\text{O}$ and hydrolysis of neodymium chloride. The general reaction is:



3.3. $\text{SmCl}_3 \cdot 6\text{H}_2\text{O}$

The results of MSA of exit gases, TG and DSC measurements of $\text{SmCl}_3 \cdot 6\text{H}_2\text{O}$ are shown in Figure 8. As in the case of thermal dehydration of $\text{NdCl}_3 \cdot 6\text{H}_2\text{O}$ four endothermic peaks are detected (at 118 , 129 , 144 and $214\text{ }^\circ\text{C}$) during thermal dehydration of $\text{SmCl}_3 \cdot 6\text{H}_2\text{O}$ over the temperature range of 20 – $250\text{ }^\circ\text{C}$. DSC effects accompanied by four steps of weight loss on the TG curve (Figure 8, curves 1 and 2). The first three endothermic peaks are accompanied by the appearance of H_2O vapor (Figure 8, curve 3). In accordance with TG data, the first three steps of dehydration are described by Reactions 13–15:

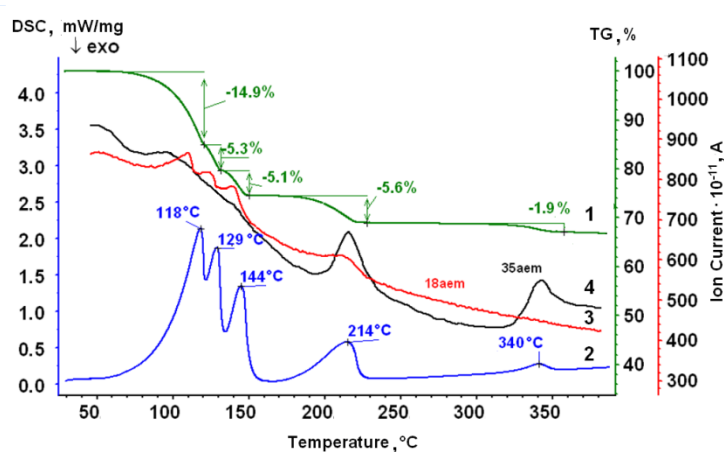
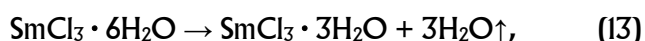
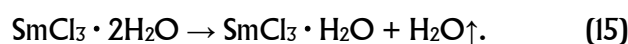
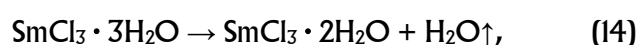
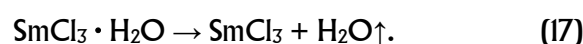
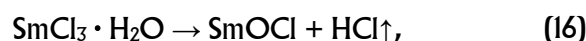


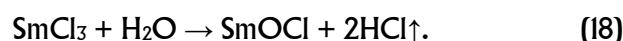
Figure 8 STA and MSA results on heating of $\text{SmCl}_3 \cdot 6\text{H}_2\text{O}$: 1 – weight, 2 – heat flow, 3 – H_2O ion current, 4 – HCl ion current.



On heating up to $214\text{ }^\circ\text{C}$, the exit of H_2O and HCl vapors is detected (Figure 8, curves 3 and 4). The corresponding Reactions are 16 and 17:

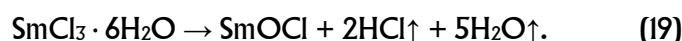


At $340\text{ }^\circ\text{C}$ a thermal effect was detected accompanied by a weight loss and the exit of HCl vapor. This proves the hydrolysis process and the formation of samarium oxychloride by Reaction 18:



Raman and IR spectra of the sample (Figure 5, curves 4 and 6) after exposure of $\text{SmCl}_3 \cdot 6\text{H}_2\text{O}$ at $500\text{ }^\circ\text{C}$ under Ar atmosphere demonstrate vibration modes of SmOCl [30, 31] (cm^{-1}): $118 - A_{1g}$; $181 - A_{1g}$; $228 - E_g$; $360 - B_g$; $489 - E_g$; $394 - A_{2u}$; $539 - E_u$. The vibration bands related to residual impurities of $\text{SmCl}_3 \cdot \text{H}_2\text{O}$, adsorbed or crystallized H_2O , and HCl not detected. The formation of samarium oxychloride was confirmed by XRD analysis of the sample obtained by the same procedure.

The general reaction is:



When comparing the thermal behavior of samarium and neodymium chloride hydrates, we note their

similarity: the same number of dehydration steps and the set of chemical reactions, the composition of intermediate and final products; the phase transformation temperatures are close.

3.4. $\text{YbCl}_3 \cdot 6\text{H}_2\text{O}$

Figure 9 shows STA and MSA data obtained on heating hydrate $\text{YbCl}_3 \cdot 6\text{H}_2\text{O}$. Over the temperature range of 20–250 °C four steps of the weight loss accompanied by endothermic effects at 152, 177, 198 and 218 °C and the exit of H_2O vapor are noted (Figure 9, curves 1, 2, 3).

In contrast to hydrates discussed above a peculiarity of the thermal behavior of $\text{YbCl}_3 \cdot 6\text{H}_2\text{O}$ is the appearance of HCl vapor (Figure 9, curve 4) even at the second dehydration step (177 °C). The reason is that the beginning of the hydrolysis process at lower temperatures as compared to $\text{NdCl}_3 \cdot 6\text{H}_2\text{O}$, $\text{SmCl}_3 \cdot 6\text{H}_2\text{O}$ and $\text{LaCl}_3 \cdot 7\text{H}_2\text{O}$ hydrates (193, 214 and 300 °C, respectively). According to STA and MSA data (Figure 9), the first step of dehydration is described by the Reaction 20:



The second, third and fourth steps of the dehydration process are accompanied by hydrolysis. Processes are described by Reactions 21–23:

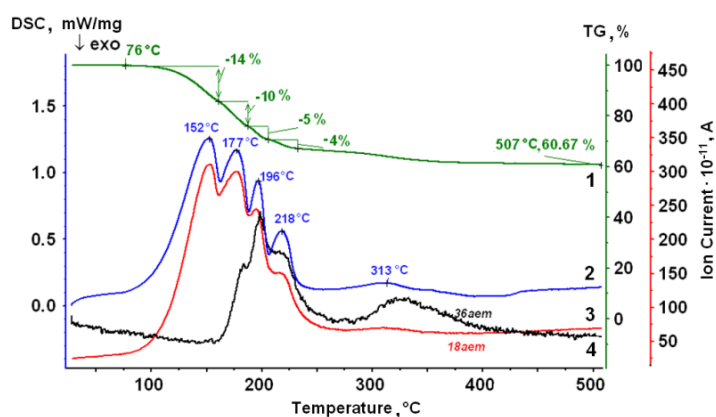
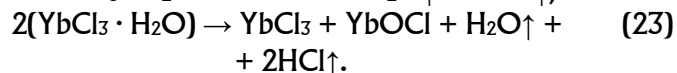
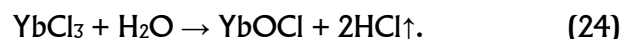


Figure 9 STA and MSA results on heating of $\text{YbCl}_3 \cdot 6\text{H}_2\text{O}$ hydrate: 1 – weight, 2 – heat flow, 3 – H_2O ion current, 4 – HCl ion current.

With further heating of the sample a stepwise weight loss was recorded over the temperature range of 250–400 °C. An endothermic effect with a maximum at 313 °C and the exit of HCl vapor (Figure 9, curves 2 and 4) was detected. This proves the interaction of ytterbium chloride with water vapor and the formation of oxychloride YbOCl by the Reaction 24:



The production of ytterbium oxychloride as a result of the thermal dehydration of $\text{YbCl}_3 \cdot 6\text{H}_2\text{O}$ was confirmed by XRD analysis, Raman and IR spectroscopy. According to the XRD data (Figure 10), the final product is YbOCl compound. No impurities of intermediate phases formed during thermal dehydration were detected. The Raman and IR spectra of the sample show (Figure 11) vibration modes of YbOCl [31–33] (cm^{-1}): 85 – E_g ; 139 – A_{1g} ; 154 – E_g ; 265 – A_{1g} ; 502 – E_g ; 533 – A_{1g} ; 391 – A_{2u} ; 426 – E_u ; 543 – A_{2u} ; 607 – E_u . No vibration bands related to residual impurities of hydrates, or HCl were detected.

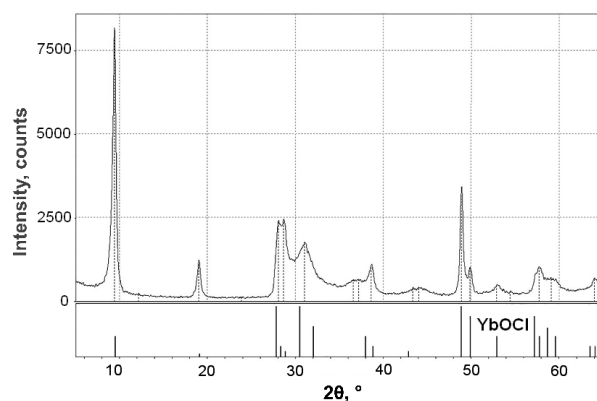


Figure 10 XRD analysis of the sample after 3-hour exposure of $\text{YbCl}_3 \cdot 6\text{H}_2\text{O}$ at 550 °C under Ar atmosphere. Formation of the YbOCl is detected.

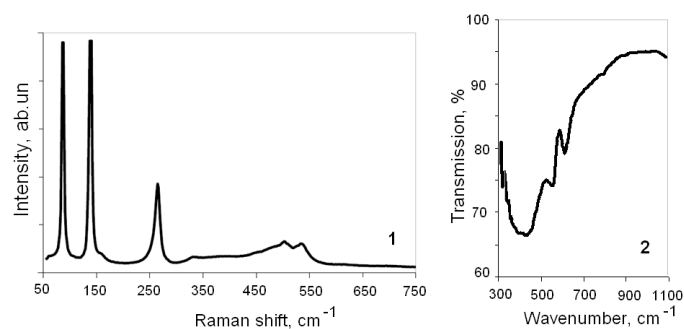
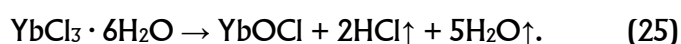


Figure 11 Raman (1) and IR (2) spectra of the sample after 3-hour exposure of $\text{YbCl}_3 \cdot 6\text{H}_2\text{O}$ hydrate at 550 °C under Ar atmosphere. Only vibration modes of YbOCl are presented.

The general reaction is:



Thus, hydrolysis of hydrate $\text{YbCl}_3 \cdot 6\text{H}_2\text{O}$ begins at 177 °C. This is the lowest temperature of the onset of hydrolysis for the studied *REM* chlorides hydrates. This feature of the thermal behavior of ytterbium chloride hydrate must be taken into account when obtaining anhydrous salt and during technological processes with its participation.

4. Conclusions

Rare earth metals are widely used in various fields of production, technology, and medicine. The development of the electrochemical synthesis of *REMs* using molten chlorides is of high relevance. Chlorides of rare earth metals are hygroscopic and actively form hydrates. The presence of impurities has a negative impact on both the process of electrolysis of melts and the yield of the target product.

By applying TG, DSC, MSA, XRD, Raman and IR spectroscopy, comprehensive studies of the thermal dehydration process of hydrates $\text{LaCl}_3 \cdot 7\text{H}_2\text{O}$, $\text{NdCl}_3 \cdot 6\text{H}_2\text{O}$, $\text{SmCl}_3 \cdot 6\text{H}_2\text{O}$ and $\text{YbCl}_3 \cdot 6\text{H}_2\text{O}$ were carried out. Distinctions in the thermal behaviors of the studied hydrates were found. Thermal dehydration of lanthanum chloride hydrate proceeds by the following scheme: $\text{LaCl}_3 \cdot 7\text{H}_2\text{O} \rightarrow \text{LaCl}_3 \cdot 3\text{H}_2\text{O} \rightarrow \text{LaCl}_3 \cdot \text{H}_2\text{O} \rightarrow \text{LaCl}_3$. Lanthanum chloride hydrolyzes and turns into LaOCl at temperatures above 300 °C in the presence of water vapor.

The hydrates $\text{NdCl}_3 \cdot 6\text{H}_2\text{O}$ and $\text{SmCl}_3 \cdot 6\text{H}_2\text{O}$ exhibit similar thermal behavior. The dehydration scheme is: $\text{REMCl}_3 \cdot 6\text{H}_2\text{O} \rightarrow \text{REMCl}_3 \cdot 3\text{H}_2\text{O} \rightarrow \text{REMCl}_3 \cdot 2\text{H}_2\text{O} \rightarrow \text{REMCl}_3 \cdot \text{H}_2\text{O} \rightarrow \text{REMCl}_3 + \text{REMOCl}$ (*REM* = Nd, Sm). In this case, hydrolysis occurs during the monohydrate dehydration at 193 and 214 °C, respectively. Hydrate $\text{YbCl}_3 \cdot 6\text{H}_2\text{O}$ is the most susceptible to hydrolysis among the studied ones. Thermal dehydration proceeds according to the following scheme: $\text{YbCl}_3 \cdot 6\text{H}_2\text{O} \rightarrow \text{YbCl}_3 \cdot 3\text{H}_2\text{O} \rightarrow \text{YbCl}_3 \cdot 2\text{H}_2\text{O} + \text{YbOCl} \rightarrow \text{YbCl}_3 \cdot \text{H}_2\text{O} + \text{YbOCl} \rightarrow \text{YbCl}_3 + \text{YbOCl}$. The production of ytterbium oxychloride occurs during the $\text{YbCl}_3 \cdot 3\text{H}_2\text{O}$ trihydrate dehydration at 177 °C. This is the lowermost hydrolysis temperature among the studied hydrates.

Comprehensive studies of the process of thermal dehydration of lanthanum, neodymium, samarium and ytterbium chloride hydrates have shown that when *REM*

chloride hydrates are heated, the removal of crystallization water is accompanied by hydrolysis, which leads to the formation of oxychloride impurities.

To obtain anhydrous *REM* chlorides, additional actions are necessary to prevent hydrolysis processes. Possible solutions are described in [34].

Supplementary materials

No supplementary materials are available.

Funding

This research had no external funding.

Acknowledgments

XRD analysis and Raman spectra were performed using the equipment of the Shared Access Centre "Composition of compounds", IHTE, Ural Branch of RAS.

Author contributions

Irina Zakiryanova: Conceptualization; Methodology; Investigation; Data curation; Writing – Review & Editing.

Iraida Korzun: Methodology; Investigation; Data curation; Writing – Original draft.

Emma Vovkotrub: Investigation.

Boris Antonov: Investigation.

Conflict of interest

The authors declare no conflict of interest.

Additional information

Irina Zakiryanova, Scopus Author ID: [36150236500](https://orcid.org/0000-0003-4513-2499); <https://orcid.org/0000-0003-4513-2499>;

Iraida Korzun, Scopus Author ID: [6603203721](https://orcid.org/0000-0002-0901-6477); <https://orcid.org/0000-0002-0901-6477>;

Emma Vovkotrub, Scopus Author ID: [6602135202](https://orcid.org/0000-0002-9610-2129); <https://orcid.org/0000-0002-9610-2129>;

Boris Antonov, Scopus Author ID: [7003392675](https://orcid.org/0000-0001-6793-1561); <https://orcid.org/0000-0001-6793-1561>.

References

- Zhang QY, Huang XY, Recent progress in quantum cutting phosphors, *Progress Mat. Sci.*, **55(5)** (2010) 353–427. <https://doi.org/10.1016/j.pmatsci.2009.10.001>
- Xu D, Zhang Y, Zhang D, Yang S, Structural, luminescence and magnetic properties of $\text{Yb}^{3+}\text{-Er}^{3+}$ codoped Gd_2O_3 hierarchical architectures, *Eng. Comm.*, **17(5)** (2015) 1106–1114. <https://doi.org/10.1039/C4CE01970A>

3. Gupta CK, Krishnamurthy N. Extractive Metallurgy of Rare Earths. London. New York. Washington: CRC PRESS; 2005. 522 p.
4. Kodina GE, Kulakov VN, Sheino IN, Rare earth elements in nuclear medicine (review). *Saratov J. Med. Sci. Res.* [Internet], **10(4)** (2014) 849–858. Russian. Available from: https://www.ssmi.ru/system/files/2014_04-01_849-858.pdf
5. Ji N, Zhu T, Peng H, Jiang F, et al., The Electrolytic Reduction of Gd_2O_3 in $LiCl-KCl-Li_2O$ Molten Salt, *Electrochem. Soc.*, **168** (2021) 082512. <https://doi.org/10.1149/1945-7111/ac1f59>
6. Liu K, Liu Y-L, Yuan L-Y, Zhao X-L, et al. Electroextraction of gadolinium from Gd_2O_3 in $LiCl-KCl-AlCl_3$ molten salts, *Electrochim. Acta*, **109** (2013) 732–740. <https://doi.org/10.1016/j.electacta.2013.07.084>
7. Guo X. Dissolution and Electrochemical Reduction of Rare Earth Oxides in Fluoride Electrolytes (dissertation) (TU Delft), Delft University of Technology; 2021. 188 p. <https://doi.org/10.4233/uuid:79a1f6f1-52d1-48a9-a0df-03c1b1ce0ac6>
8. Wendlandt W, The thermal decomposition of yttrium, scandium, and some rare-earth chloride hydrates, *J. Inorg. Nucl. Chem.*, **5(2)** (1957) 118–122. [https://doi.org/10.1016/0022-1902\(57\)80052-9](https://doi.org/10.1016/0022-1902(57)80052-9)
9. Wendlandt W. The thermal decomposition of the heavier rare earth metal chloride hydrates, *J. Inorg. Nucl. Chem.*, **9(2)** (1959) 136–139. [https://doi.org/10.1016/0022-1902\(59\)80072-5](https://doi.org/10.1016/0022-1902(59)80072-5)
10. Korzun IV, Zakir'yanova ID, Nikolaeva EV, Mechanism and Caloric Effects of the Thermal Dehydration of $GdCl_3 \cdot 6H_2O$ Crystalline Hydrate, *Russian Metallurgy (Metally)*, **2018** (2018) 722–727. <https://doi.org/10.1134/S0036029518080104>
11. Zakiryanova ID, Zakiryanov DO, Zakiryanov PO, Local structure and dynamics of ions in $LiCl-GdCl_3$, $KCl-GdCl_3$ and $LiCl-GdCl_3-Gd_2O_3$ melts: Ab initio molecular dynamics simulations and Raman spectroscopy, *J. Mol. Liq.*, **376** (2023), 121485. <https://doi.org/10.1016/j.molliq.2023.121485>
12. Nikolaeva EV, Zakiryanova ID, Bovet AL, Korzun IV, Electrical conductivity of $GdCl_3-LiCl$ and $GdCl_3-LiCl-Gd_2O_3$ molten systems, *J. Serb. Chem. Soc.*, **88(11)** (2023) 1135–1147. <https://doi.org/10.2298/JSC230131051N>
13. Zakiryanov D, The impact of oxide impurity on the structure of $FLiNaK$ and $FLiNaK-CeF_3$ melts: A simulation study, *J. Mol. Liq.*, **384** (2023) 122265. <https://doi.org/10.1016/j.molliq.2023.122265>
14. Zakiryanov DO, Zakiryanova ID, Tkachev NK, Study of local structure and ion dynamics in $GdCl_3-Gd_2O_3$ and $KCl-GdCl_3-Gd_2O_3$ melts: In situ Raman spectroscopy and ab initio molecular dynamics, *J. Mol. Liq.*, **301** (2020) 112396 <https://doi.org/10.1016/j.molliq.2019.112396>
15. Korzun IV, Nikolaeva EV, Zakir'yanova ID, Thermal analysis of the oxide-chloride systems $GdCl_3-Gd_2O_3$ and $GdCl_3-KCl-Gd_2O_3$, *J. Thermoanal. Calorim.*, **144** (2020) 1343–1349. <https://doi.org/10.1007/s10973-020-09558-2>
16. Ashcroft SJ, Mortimer CT, The thermal decomposition of lanthanide (III) chloride hydrates, *J. Less-Com. Met.*, **14(4)** (1968) 403–406. [https://doi.org/10.1016/0022-5088\(68\)90164-1](https://doi.org/10.1016/0022-5088(68)90164-1)
17. Sokolova NP, Ukraintseva EA, Dissociation pressure of some crystalline hydrates of lanthanide chlorides, *Izv. Siberian Branch of the USSR Acad. Sci. Ser. chem. sci.*, **3** (1984) 24–26. Russian.
18. Ukraintseva EL, Sokolova NP, Logvinenko VA, Thermodynamic characteristics of dehydration of hepta- and hexahydrates of lanthanide chlorides of the cerium subgroup. *Radiochem.*, **29** (1987) 481–485. Russian.
19. Ukraintseva EA, Sokolova NP, Logvinenko VA, Thermodynamic characteristics of dehydration of erbium, thulium and lutetium chloride hexahydrates. *Radiochem.*, **31** (1991) 78–80. Russian.
20. Haeseler G, Matthes F, Uber den thermischen Abbau dek Chloridhydrate der Elemente der seltenen erden, *J. Less-Comm. Met.*, **9(2)** (1965) 133–151. [https://doi.org/10.1016/0022-5088\(65\)90090-1](https://doi.org/10.1016/0022-5088(65)90090-1)
21. Hong VV, Sundstrum J, The dehydration schemes of rare-earth chlorides, *Thermochim. Acta.*, **307(1)** (1997) 37–43. [https://doi.org/10.1016/S0040-6031\(97\)00296-7](https://doi.org/10.1016/S0040-6031(97)00296-7)
22. Lee T, Cho Y, Eun H, Son S, et al. A study on dehydration of rare earth chloride hydrate, *J. Korean Radioactive Waste Soc.*, **10(2)** (2012) 125–132. <https://doi.org/10.7733/JKRWS.2012.10.2.125>
23. Kipouros GJ, Sharma RA, Characterization of neodymium trichloride hydrates and neodymium hydroxychloride, *J. Less-Com. Met.*, **160(1)** (1990) 85–99. [https://doi.org/10.1016/0022-5088\(90\)90110-6](https://doi.org/10.1016/0022-5088(90)90110-6)
24. Sundstrum J, Hong VV, Investigation of the kinetics of the fluidized bed process for the dehydration of $NdCl_3 \cdot 6H_2O$, $TbCl_3 \cdot 6H_2O$ and $DyCl_3 \cdot 6H_2O$. *Thermochim. Acta.*, **306(1–2)** (1997) 13–21. [https://doi.org/10.1016/S0040-6031\(97\)00293-1](https://doi.org/10.1016/S0040-6031(97)00293-1)
25. Sahoo DK, Thakur S, Mishra R, Determination of thermodynamic stability of neodymium chloride hydrates ($NdCl_3 \cdot xH_2O$) by dynamic transpiration method, *J. Therm. Anal. Calorim.*, **126** (2016) 1407–1415. <https://doi.org/10.1007/s10973-016-5714-1>
26. Grasselli JG, Snavely MK, Balkin BJ. Chemical applications of Raman Spectroscopy. N. York. Toronto: Wiley Publ.; 1973. 216 p.
27. Kochedykov VA, Zakiryanova ID, Akashev LA, Identification of products of interaction of oxides of rare earth metals with components of the air atmosphere using IR spectroscopy, *Analytics and control*, **10** (2006) 172–174. Russian. URI: <http://elar.urfu.ru/handle/10995/58134>
28. Kochedykov VA, Zakiryanova ID, Korzun IV, Study of the thermal decomposition of the products of interaction of rare earth oxides with components of the air atmosphere, *Analytics and control*, **9** (2005) 58–63. Russian. URI: <http://elar.urfu.ru/handle/10995/58914>
29. Makatun VN. Chemistry of inorganic hydrates. Moscow: Science and Technology; 1985. 245 p. Russian.
30. Hase Y, Dunstan POL, Temperini MLA, Raman active normal vibrations of lanthanide oxychlorides, *Spectrochim. Acta. Part A: Mol. Spectroscopy*, **37(8)** (1981) 597–599. [https://doi.org/10.1016/0584-8539\(81\)80055-4](https://doi.org/10.1016/0584-8539(81)80055-4)
31. Basile LJ, Ferraro JR, Gronert D, I.R. Spectra of several lanthanide oxyhalides, *J. Inorg. Nuclear Chem.*, **33(4)** (1971) 1074–1053. [https://doi.org/10.1016/0022-1902\(71\)80173-2](https://doi.org/10.1016/0022-1902(71)80173-2)
32. Zakiryanova ID, In situ Raman Spectroscopic Study of the Kinetics of the Chemical Dissolution of Ytterbium Oxide in $YbCl_3-KCl$ Melt, *J. Appl. Spec.*, **88** (2021) 755–760. <https://doi.org/10.1007/s10812-021-01236-x>

33. Zakiryanova ID, Zakiryyanov DO, Ab initio molecular dynamics simulations and Raman spectra of the YbCl_3 -KCl and Yb_2O_3 - YbCl_3 -KCl ionic melts, *J. Mol, Liq*, **318** (2020) 114054. <https://doi.org/10.1016/j.molliq.2020.114054>

34. Revzin GE, Anhydrous chlorides of rare earth elements and scandium. In: *Methods of Obtaining of Chemical Reagents and Preparations*. Moscow: Science and Technology; 1967. p. 16–27. Russian.